J. Chil. Chem. Soc., 58, Nº 4 (2013)

SYNTHESIS AND STRUCTURAL CHARACTERIZATION OF NANOCRYSTALLINE BATIO$_3$ AT VARIOUS CALCINATION TEMPERATURES

SANDRA FUENTES[1,6], FRANCISCO CÉSPEDES[2], PAMELA MUÑOZ[3], EMIGDIO CHÁVEZ[4] AND LUIS PADILLA-CAMPOS[5]*

[1]*Departamento de Ciencias Farmacéuticas, Facultad de Ciencias, Universidad Católica del Norte Casilla 1280, Antofagasta, Chile.*
[2]*Departament de Física, Facultad de Ciencias, Universidad Católica del Norte, Casilla 1280, Antofagasta, Chile.*
[3]*Departamento de Química, Facultad de Ciencias, Universidad Católica del Norte Casilla 1280, Antofagasta Chile.*
[4]*Catalan Institute of Nanotechnology (CIN2-CSIC), Campus Universitat Autònoma de Barcelona, Bellaterra 08193, Spain.*
[5]*Departamento de Química, Facultad de Ciencias Básicas, Universidad de Antofagasta, Casilla 170, Antofagasta, Chile.*
[6]*Center for the Development of Nanoscience and Nanotechnology,CEDENNA, Santiago, Chile.*
(Received: July 30, 2013 - Accepted: August 22, 2013)

ABSTRACT

Barium titanate ($BaTiO_3$) powders with particle sizes about 50 nm in diameter were synthesized using a hydrothermal route. The powders were characterized using various experimental techniques such as XRD, TEM and Raman spectroscopy, and they showed a good crystallinity and homogeneity without heat treatments. Also, Raman spectra showed the presence of the tetragonal phase. In addition, various calcination treatments were made to $BaTiO_3$ powders with the purpose to improve their ferroelectric properties. In general, calcination treatments improved the crystallinity and homogeneity of the samples considerably but did not modify the internal structure of the $BaTiO_3$, which was observed in the Raman spectra. On the other hand, from theoretical calculations were established that the cubic phase should be better dielectric in comparison with the tetragonal phase, but this latter would have better optical properties. However, experimental evidences are indicative that the cubic phase would predominate in the synthesis of the compound.

Keywords: $BaTiO_3$, nanoparticles, hydrothermal synthesis, Raman spectroscopy, X-ray diffraction, Transmission electron microscopy, theoretical calculations.

1. INTRODUCTION

Interest in the synthesis of nanoparticles of ferroelectric materials has been on the increase over time due to the need for miniaturization of electronic devices thanks to the technology industry. Barium titanate (BTO) is one of the materials being investigated for this purpose, owing to its ferroelectric properties such as high dielectric constant and large polarization per unit cell that arises from an asymmetric displacement of oxygen and titanium ions along the polar axis. This results in a net dipole moment, which depends directly on the extension that has distorted the axes in the tetragonal phase. This distortion is small (approximately 1% ((c-a)/a), and therefore, a fine structural characterization is crucial, especially considering the fact that the ferroelectric polarization in BTO decreases with the decreasing particle size [1-3]. X-ray diffraction is often used to structurally characterize areas of particles as it is ideal for differentiating phase changes in compounds such as BTO. However, this technique is unsuitable for the characterization of very small particles due to the extensive broadening of Bragg reflections. Also, this technique is not very sensitive to transitions which involve displacement of oxygen [4]. The characterization techniques based on the crystal symmetry, such as the Raman spectroscopy can detect crystallographic distortions and defects at the molecular level [5]. In the case of BTO it has been demonstrated theoretically that the technique is able to detect distortions in the order of 0.5 pm [6].

For the synthesis of a pure, homogeneous and nanometric level of BTO, wet chemical routes have been used, which have huge economic advantages over the conventional manufacturing methods (solid-solid reaction) [7-9]. As an alternative, Raman spectroscopy is a powerful experimental tool for studying the lattice vibrations and other elementary excitations in materials, providing important information about the structure, composition, strain, defects, and phase transitions. The Raman spectra of the BTO nanoparticles can detect the presence of tetragonal phase of particles as small as those between 20 to 150 nm [10,11].

Busca *et al.* [12] reported a distortion of the TiO_6 octahedron in the cubic BTO phase inducing a pseudotetragonality of the cubic phase. This could explain the significantly lower symmetry with respect to a cubic perovskite structure, similar to that of the tetragonal BTO.

Taking into account the benefits of wet routes for the synthesis of BTO and a high sensitivity to the symmetry of Raman spectroscopy as was established in a previous paper [6], the goal of the present work is to study the BTO nanoparticles obtained by the sol-gel hydrothermal synthesis method, as well as to study the changes in the nanoparticles and their effects at different times and calcination temperatures, characterizing them by means of various experimental techniques, such as XRD and TEM, and fundamentally by means of Raman spectroscopy. In addition, from theoretical calculations the electronic structure will be obtained for both, tetragonal and cubic phases, to establish general properties that characterize both phases.

2. EXPERIMENTAL

Nanocrystalline BTO powders were prepared by a sol-gel-hydrothermal reaction of $TiCl_4$ and a $BaCl_2$ solution in an oxygen atmosphere. The colloidal mixed solution was transferred into a 500 mL Teflon-lined stainless autoclave and heated at two temperatures (180 and 220 ºC) for 3 and 24 h under an oxygen partial pressure of 60 bar. At the end of the reaction, the autoclave was naturally cooled to room temperature. The as-formed solid white powder attached to the bottom and inner wall of the Teflon container was collected, centrifuged, washed with distilled water and ethanol to remove remaining ions, and dried at 60 ºC for 6 h under vacuum. For all samples, the calcination treatment was performed at 250, 300, 350, 400, and 500 ºC for 3, 6, and 12 h, respectively at the rate of 10°/min.

The samples obtained were analyzed by X-ray diffraction (XRD) using a Siemens D5000 diffractometer with CuK_α radiation (40 kV, 30 mA). Transmission electron microscopy (TEM) studies were performed in a Tencai F20 FEG-TEM operated at 200 kV, equipped with an EDS detector. The TEM samples were ultrasonically dispersed in isopropanol and then collected in a carbon grid. The Raman spectra were recorded on a WITEC model CRC200, using a 5.5 mW laser with a wavelength of 514.5 nm.

2.1. RESULTS AND DISCUSSION

Figure 1 shows the X-ray powder diffraction pattern of the solid product before calcinations. The well-resolved peaks revealed good crystallinity of the obtained $BaTiO_3$ powder samples not subjected to any heat treatment. On the

e-mail: lpadilla@uantof.cl

right side of Figure 1 are the XRD patterns in the 2θ regions of 44–46º. The absence of diffraction peak splitting in (200) shows the presence of a cubic structure for these BTO powders at room temperature. According to JCPDS cards the single peak (200) can be indexed as the cubic lattice (space group *Pm3m*) of BTO and the calculated lattice constants are in good agreement with the tabulated values (JCPDS cards No. 31-0174). This implies that the particles are apparently stabilized in the cubic phase at room temperature. In addition, with an increase in the reaction time, i.e. at 24 h, all the peaks became much sharper than at 3 h in the diffractogram. The XRD patterns of the calcined samples are not shown because they did not show any significant changes in the crystallinity.

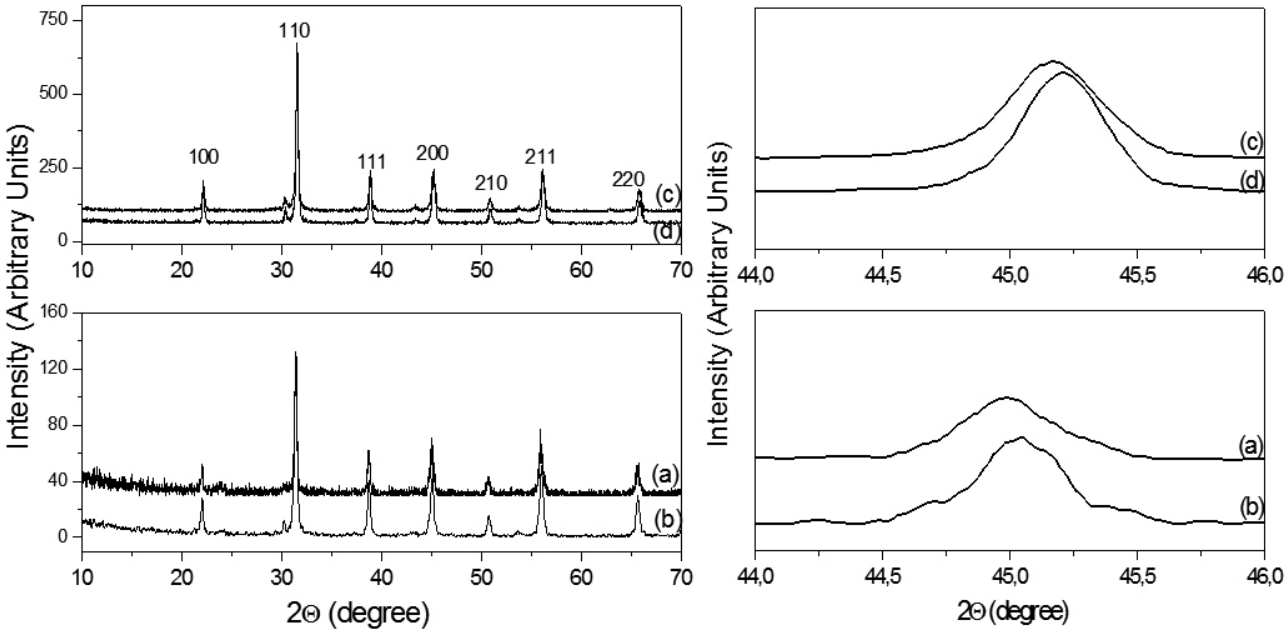

Figure 1. XRD patterns of the product obtained with different reaction temperatures an time: (a) 180°C/3h, (b) 220°C/3h, (c) 180°C/24h and (d) 220°C/24h. The right side shows the XRD patters in the 2θ region among 44 and 46°.

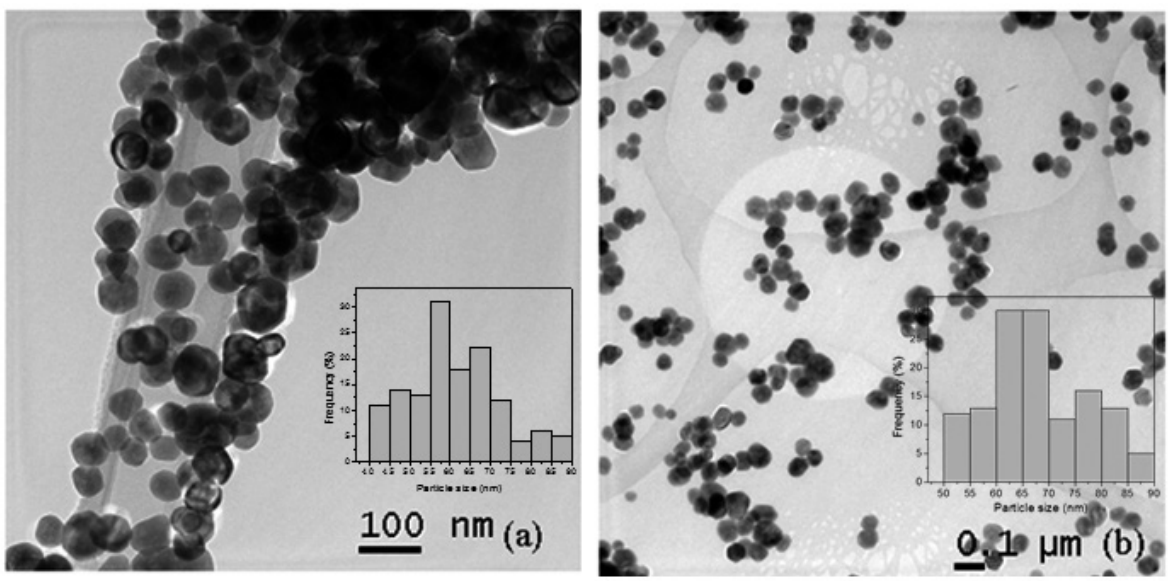

Figure 2. TEM image of the $BaTiO_3$ nanoparticles obtained at 220°C and 24 h. (a) without calcination and (b) calcined at 300°C for 12 h. The insets are their corresponding particle size distribution histograms.

Figure 2 shows the TEM micrographs of the BTO powders synthesized after 24 h of reaction at 220 ºC with and without calcinations. With regard to samples without calcinations, the particles appear to have a fairly narrow size from 40 to 90 nm with a preferred size of about 57 nm (Figure 2a and the inset). The TEM image of the calcined samples at 300 ºC for 12 h is shown in Figure 2b and the inset. In addition, the image indicates that coarser faceted particles are apparent in the powder with calcinations and a bimodal distribution of larger faceted particles presents an increase of the particle size about 65 nm. This result indicates that most of the crystallites of BTO adhere together and form large particles. Nearly all particles are elliptical in shape, well dispersed with a slight agglomeration.

BTO single crystals at room temperature have a tetragonal perovskite structure (space group *P4mm*) with one formula unit per unit cell. Only below the Curie point, near 120 ºC, does BTO become ferroelectric. During the interval of 120–1460 ºC, BTO monocrystals take the paraelectric cubic perovskite structure (space group *Pm3m*).

As it is known, Raman spectroscopy is a highly sensitive technique to probe the local structure of BTO samples [6,13,14]. Figure 3 shows the Raman spectra of BTO samples under different times of calcination. This heat treatment raises the temperature and allowed to decompose impurities from the synthesis (e.g., $BaCO_3$), structural defects and oxygen vacancies. Therefore, BTO samples were calcinated to improve the crystallinity, homogeneity and purity of the synthesized samples. Raman results of all samples prepared under calcinations (Figure 3 a, b and c) show a small gradual increase in the peaks, characteristic of active modes of the tetragonal phase of BTO when the temperature increases and calcination time is constant. These bands are about 175 cm^{-1} [A1(TO), E(LO)] and 307 cm^{-1} [B1, E(TO+LO)] and broad bands around 265 cm^{-1} [A1(TO)], 520 cm^{-1} [A1, E(TO)], and 720 cm^{-1} [A1, E(LO)]. The appearance of strong Raman peaks near 307 cm^{-1} (B1 mode) that corresponds to tetragonal BTO phase is contradictory with the cubic symmetry observed in the XRD analysis, for which no first-order Raman activity is expected. This apparent contradiction was resolved in our previous work [6] where we showed using theoretical calculation within the Density Functional Theory framework that the Raman spectroscopy is a technique highly sensitive to the molecular level, being able to detect distortion about 0.5 pm in the crystalline structure of BTO.

A more exhaustive analysis of Raman spectra in Figure 3 shows slight differences between them, indicating that the uncalcined samples are fairly homogeneous and crystalline and the calcinations did not modify the internal structure of the BTO which is reflected in the spectra. The most significant increase in the intensity of the band at 307 cm^{-1} is shown in Figure 3b. In general, the peaks are sharper at low temperatures, and begin to widen with increasing temperatures. This would either indicate that there are particles belonging to cubic phase or denote small structural defects. With the help of thermal activation of these crystals, the particles quickly approached the tetragonal phase. As the temperature is rising, the nucleation process prevents the cubic phase transition to tetragonal and generates a low-symmetry cubic phase.

3. Theoretical calculations

To characterize the cubic and tetragonal phases of BTO, we proceeded to carry out quantum chemical calculations to obtain the electronic structure and density of state, local and total, in both phases. To simulate both phases the cluster methodology [15-18] was used, i.e., a finite number of atoms were used to represent the different phases. The cluster consisted in eight unit cells, representing to both phases. Crystallographic data were used to build the cubic and tetragonal clusters reported in the literature [14,19]. Electronic properties have been calculated by solving the Kohn–Sham equations in an atomic basis set formed by Gaussian functions. The calculations have been done using the B3LYP exchange correlation functional [20-23], which is of the hydrid type. For titanium and oxygen atoms the 6-31G basis set [24,25] has been used. For barium atoms the pseudopotential of the Los Alamos group [26] with a corresponding basis set has been used. The pseudopotential replaces 54 core electrons thus only two valence electrons are considered. All calculations were done using the Gaussian 09 program [27].

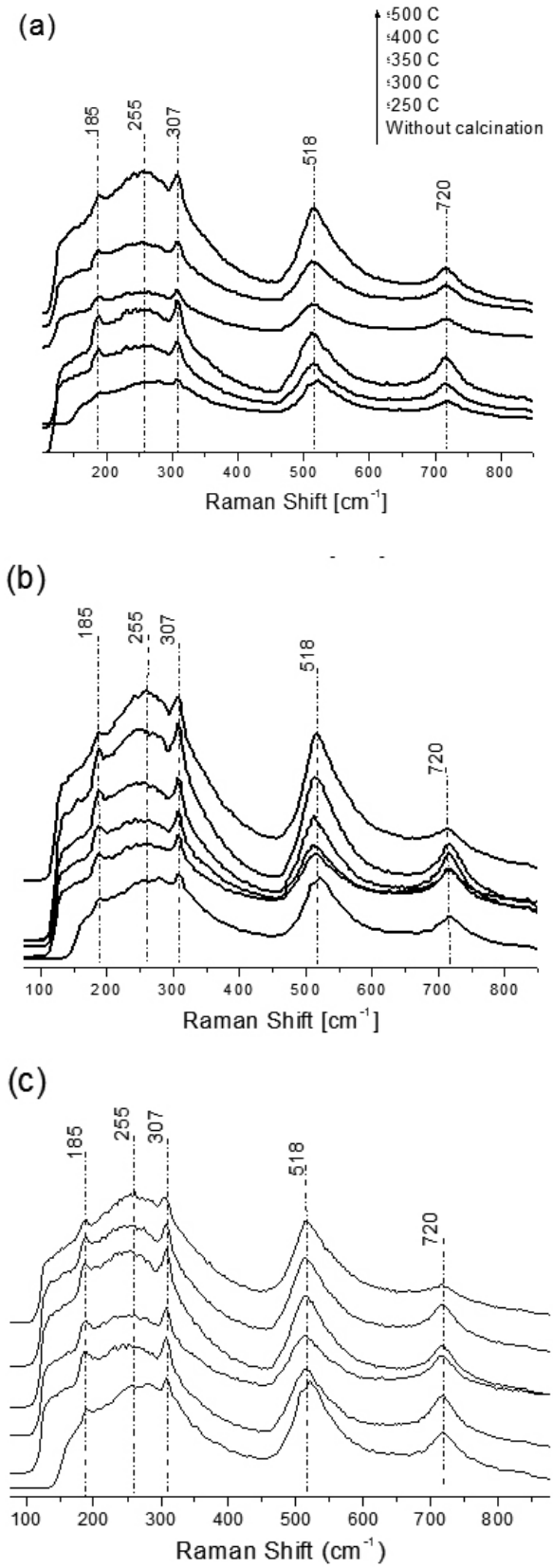

Figure 3. Raman spectra of the sample obtained at 220 °C and 24 h under different time of calcinations: (a) 3 h, (b) 6 h and (c) 12 h.

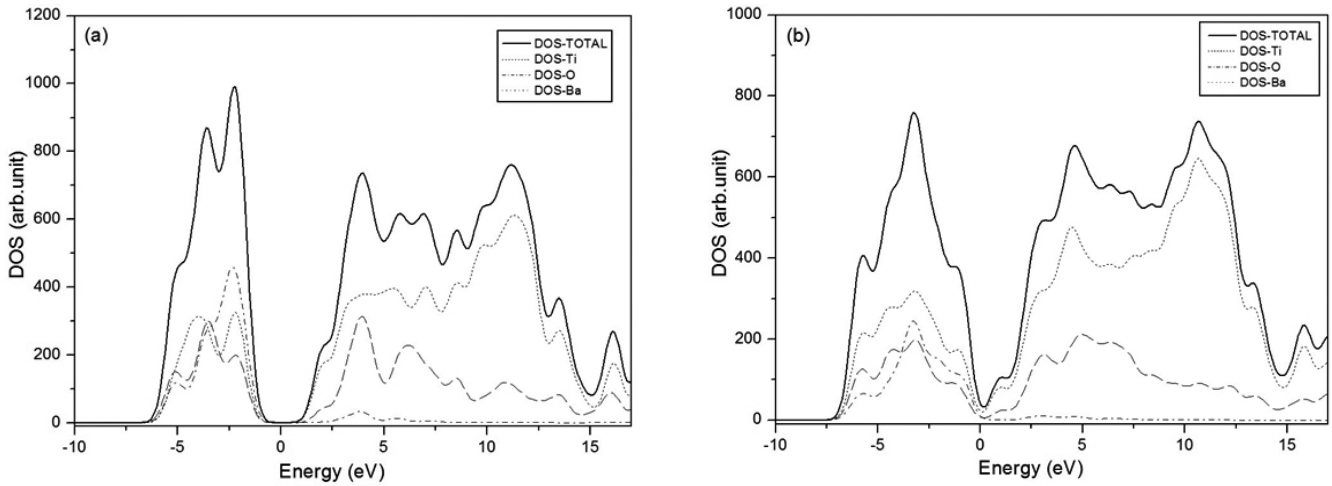

Figure 4. Density of States for $BaTiO_3$: (a) cubic and (b) tetragonal phases.

3.1. RESULTS AND DISCUSSION

Density of states for cubic and tetragonal phases is shown in Fig. 4. The percentage of elemental contribution is shown in Table 1. The analysis of the density of states show that in the cubic phase the main contributions in the valence band (VB) are oxygen and barium atoms (about 37%) following by the Ti atom. In change, in the tetragonal phase the main contributions are Ba (about 48%), following by Ti and O atoms. For the conduction band (CB) the main contribution in both phases is the Ba atom, about 75% and 77% for cubic and tetragonal phases, respectively. The above results are indicative, in general, that the transition of the cubic phase to the tetragonal phase favors the contribution of the Ba atom to the VB without affecting the CB.

Table 1. Percentage of elemental contribution to the density of states for the cubic and tetragonal phases of $BaTiO_3$. Valence Band (VB) and Conduction Band (CB).

	Cubic		Tetragonal	
Element	VB	CB	VB	CB
Ti	27.1	23.8	26.3	22.6
O	36.5	1.1	25.9	0.6
Ba	36.4	75.1	47.8	76.8

In Table 2 are displayed the percentage of elemental contribution at the top and background of the VB and CB, respectively. As we can see the main contribution at the top of the BV is the O atom (about 95%) in the cubic phase. In change, in the tetragonal phase the O contribution decrease at about 42% in comparison to the cubic phase, increasing the contribution of the Ba atom at about 47%. For the CB the main contribution is the Ba atom (higher than 83%) for both phases.

The theoretical gap (energy difference among the VB and the CB) for cubic phase was 3.42 eV, which is according to the experimental value of 3.4 eV [28]. The theoretical gap for the tetragonal phase decrease to about 1.50 eV. These results are indicative that dielectric properties could decrease in the latter phase.

In a recent work [29] was shown that the tetragonal distortion does not change significantly the charge distribution neither the energetic stability of the compound. Thus, the theoretical calculation are indicating that tetragonal distortion tend to modify the optical and dielectric properties of the compound, affecting mainly the gap of the compound changing the elemental contribution in the VB, while the CB is not affected.

Table 2. Percentage of elemental contribution to the density of states for the cubic and tetragonal phases of $BaTiO_3$ at the top of the Valence Band (VB) and background of the Conduction Band (CB).

	Cubic		Tetragonal	
Element	BV	BC	BV	BC
Ti	0.0	11.9	11.1	16.2
O	95.3	3.3	41.7	0.6
Ba	4.7	84.8	47.2	83.2

4. CONCLUSIONS

Barium titanate (BTO) powders with particle sizes about 50 nm in diameter were synthesized using a sol-gel-hydrothermal process. The analysis of powders by means of experimental techniques such as XRD, TEM, and Raman spectroscopy showed a good crystallinity and homogeneity of the samples without heat treatments. Raman spectra showed the presence of the tetragonal phase, in contrast with the XRD results that showed only the presence of a cubic phase. However, this controversy was solved in a previous work [6], where it was established that Raman spectroscopy is a sensitive technique and is able to detect small distortions in the crystalline structure of the BTO and, the active mode to 307 cm^{-1} can be used to detect the presence of the tetragonal phase. In addition, various calcination treatments were made to BTO powders with the purpose to improve their ferroelectric properties. In general, the calcinations improved the crystallinity and homogeneity of the samples considerably but did not modify the internal structure of the BTO, which was observed in the Raman spectra. On the other hand, theoretical calculations showed that tetragonal phase has a minor gap in comparison to the cubic phase, indicating that the latter phase would have better dielectric properties than the former. However, the gap value determined experimentally and XRD results were according with a cubic phase, suggesting that this latter phase is present in high percentage in the synthesis of the compound. The latter result is agreement with that found by Ciftci et al. [30].

ACKNOWLEDGMENTS

This work has been partially financed by: FONDECYT Grant under contract No 1110555. Basal Financing Program CONICYT, FB0807 (CEDENNA). MICINN Project ACPHIN (FIS2009-10150). E. C. is gratefully acknowledged for fellowship from CONICYT through Becas Chile 2010. Proyectos de la Dirección de Investigación (U. de Antofagasta), Grant DI-CODEI-2010-01.

REFERENCES

1.- H. Kishi, Y. Mizuno, H. Chanzono. *Jpn. J. Appl. Phys*. **42**, 1, (2003).
2.- G. Arlt, D. Hennings, G. de UIT. *J. Appl. Phys*. **58**, 1619, (1985).
3.- Y. Shiratori, C. Pithan, J. Dornseiffer, R. Waser. *J. Raman Spectrosc*. **38**, 1288 (2007).
4.- M. Yashima, K. Ohtake, M. Kakihana, H. Arashi, M. Yoshimura. *J. Phys. Chem. Solids* **57**, 17, (1996).
5.- P.S. Dobal, R.S, Katiyar. *J. Raman Spectrosc.* **33**, 405, (2002).
6.- E. Chavez, S. Fuentes, R.A. Zarate, L. Padilla-Campos. *J.Molec.Struct.* **984,** 131, (2010).
7.- S. Wada, T. Suzuki, T. Noma. *Jpn. J. Appl. Phys.* **34**, 5368, (1995).
8.- T. Noma, S. Wada, M. Yano, T. Suzuki. *J. Appl. Phys.* **80**, 5223, (1996).
9.- S Wada, M. Yano, T. Suzuki, T Noma. *J. Mater. Sci* .**35**, 3889, (2000).
10.- S.W Lu, B.I Lee, Z.L. Wang, W.D. Samuels. *J. Cryst. Growth*, **219**, 269, (2000).
11.- Y.I Kim, J.K Jung, K.S Ryu. *Mater. Res. Bull.* **39**, 1045, (2004).
12.- G. Busca, V. Buscaglia, M. Leoni, P. Nanni. *Chem. Mater.* **6**, 955, (1994).
13.- U. Venkateswaran, V. Naik, R. Naik. *Phys Rev. B*. **58**, 14256, (1998).
14.- P. Hermet, M. Veithen, P. Ghosez. J. Phys.: Condens. Matter. **21**, 215901, (2009).
15.- T.A. Kaplan, S.D. Mahanti, Electronic Properties of Solids using Cluster Methods, Plenum Press, New York, 1995.
16.- L. Padilla-Campos, P. Fuentealba, *Theo. Chem. Acc*. **110**, 414, (2003).
17.- L. Padilla-Campos, *J. Molec. Struc. (THEOCHEM)*. **621**, 107, (2003).
18.- F. Céspedes, L.Padilla-Campos, *J. Chil. Chem. Soc.,* **57**, 1022, (2012)
19.- H. Dittrich, N. Karl, S. Kück, H.W. Schock, Ternary Compounds, organic semiconductors, Springer-Verlag; U.S.A, 2000.
20.- A.D. Becke. *J. Chem. Phys*. **98**, 5648, (1993).
21.- A.D. Becke. *Phys. Rev.A*. **38**, 3098, (1988).
22.- B. Miehlich, A. Savin, H. Stoll, H. Preuss. *Chem. Phys. Lett*. **157**, 200, (1989).
23.- C. Lee, W. Yang, R.G. Parr. *Phys. Rev. B*, **37,** 785, (1988).
24.- W.J. Hehre, R. Ditchfield, J.A. Pople*, J. Chem. Phys*. **56**, 2257, (1972).
25.- V. Rassolov, J.A. Pople, M. Ratner, T.L. Windus, *J. Chem. Phys*. **109**, 1223, (1988).
26.- P.J Hay, W.R. Wadt. *J. Phys*. ***82***, 270, (1985).
27.- M. J. Frisch, G. W. Trucks, H. B. Schlegel, G. E. Scuseria, M. A. Robb, J. R. Cheeseman, G. Scalmani, V. Barone, B. Mennucci, G. A. Petersson, H. Nakatsuji, M. Caricato, X. Li, H. P. Hratchian, A. F. Izmaylov, J. Bloino, G. Zheng, J. L. Sonnenberg, M. Hada, M. Ehara, K. Toyota, R. Fukuda, J. Hasegawa, M. Ishida, T. Nakajima, Y. Honda, O. Kitao, H. Nakai, T. Vreven, J. A. Montgomery, Jr., J. E. Peralta, F. Ogliaro, M. Bearpark, J. J. Heyd, E. Brothers, K. N. Kudin, V. N. Staroverov, T. Keith, R. Kobayashi, J. Normand, K. Raghavachari, A. Rendell, J. C. Burant, S. S. Iyengar, J. Tomasi, M. Cossi, N. Rega, J. M. Millam, M. Klene, J. E. Knox, J. B. Cross, V. Bakken, C. Adamo, J. Jaramillo, R. Gomperts, R. E. Stratmann, O. Yazyev, A. J. Austin, R. Cammi, C. Pomelli, J. W. Ochterski, R. L. Martin, K. Morokuma, V. G. Zakrzewski, G. A. Voth, P. Salvador, J. J. Dannenberg, S. Dapprich, A. D. Daniels, O. Farkas, J. B. Foresman, J. V. Ortiz, J. Cioslowski, and D. J. Fox, Gaussian 09, Revision B.01, Gaussian, Inc., Wallingford CT, 2010.
28.- E. Longo, E. Orhan, F.M. Pontes, C.D. Pinheiro, E.R. Leite, J.A Varela, P.S. Pizani, T.M. Boschi, F. Lanciotti, Jr., A. Beltran, J. Andrés, *Phys. Rev.B,* **69**, 125115, (2004).
29.- S. Fuentes, E. Chávez, L. Padilla-Campos and D.E. Diaz-Droguett, *Ceramic International*. **39**, 8823, (2013).
30.- E. Ciftci, M. Rahaman, M. Shumsky, *J. Mat. Sci*., **36**, 4875, (2001).